DANMARKS OG GRØNLANDS GEOLOGISKE UNDERSØGELSE RAPPORT 2009/51

Silica diagenesis in the EE and ED reservoir zones of the Ekofisk Formation, Ekofisk Field, Norway

Heine Buus Madsen

GEOLOGICAL SURVEY OF DENMARK AND GREENLAND
MINISTRY OF CLIMATE AND ENERGY

GEUS

DANMARKS OG GRØNLANDS GEOLOGISKE UNDERSØGELSE RAPPORT 2009/51

Silica diagenesis in the EE and ED reservoir zones of the Ekofisk Formation, Ekofisk Field, Norway

Heine Buus Madsen

GEOLOGICAL SURVEY OF DENMARK AND GREENLAND
MINISTRY OF CLIMATE AND ENERGY

GEUS

Table of content **Page**

Silica diagenesis in the EE and ED reservoir zones of the Ekofisk Formation, Ekofisk field, Norway

Madsen, H.B., Geological Survey of Denmark and Greenland, Copenhagen 1350-DK, Denmark

Summary

Diagenetic minerals are known to affect the porosity and permeability of sediments and understanding of the processes and timing for these minerals will improve reservoir models. This report focus on early diagenetic flint formation and late mineral reactions in the chalk and how these can be distinguished by petrophysical logs.

The flint layers consist mainly of microquartz and minor chalcedony, lutecite and dolomite. The flint layers were preferentially formed in the northern part of the Ekofisk Field where bottom currents were strongest and supplied nutrients, particulate matter and silica. The currents nourished siliceous sponge colonies which were the main source of silica. The presence of abundant dolomite in the chalk indicates that microbial degradation of organic matter occurred, which initiated precipitation of silica gel and opal-CT at the redox boundary in the sediment. Later phase transformations converted the gel and opal-CT to quartz.

The chalk and marls contain insoluble diagenetic minerals, including quartz, kaolinite, smectite-illite, plagioclase, fluor-apatite, crandelite, barite and pyrite. A late diagenetic mineral reaction for the formation of kaolinite and smectite-illite is suggested. During burial Mg, Fe and Si were released from the octahedral layer in detrital smectites and substituted by Al. Dissolution of feldspar contributed with Al, Si and minor K to solution from where primarily kaolinite and little smectite-illite were precipitated. Excess Si precipitated as quartz in close association with kaolinite.

The petrophysical logs GR, RHOB and NPHI are shown to be useful in tracing and correlating flint layers and levels with high silica content. Cross plots further indicate that the diagenetic precipitation of early flint and the late mineral reactions reduced porosity.

1. Introduction

Diagenetic precipitation of minerals is known to affect the porosity and permeability of sediments and knowledge of the diagenetic processes and their timing is important in order to better predict reservoir characteristics.

Several studies on diagenesis of chalk have been carried out on the North Sea oil fields (Scholle, 1977; Taylor and Lapré, 1987; Maliva et al., 1991; Maliva and Dickson, 1992; Hancock, 1993) but only few have been focused on the silica diagenesis (Jakobsen et al., 2000, Fabricius and Borre, 2006; Fabricius et al. 2007). Silica is not a major phase in the chalk but constitutes locally a major phase in some stratigraphic intervals as the lower part of the Ekofisk Formation in the Ekofisk Field. This may indicate variations in facies and palaeo-oceanography, as the silica represents diagenetically reprecipitated biogenic silica (Fabricius and Borre, 2007). High abundance of biogenic silica found in some sediment has been interpreted to indicate the presence of bottom currents and upwelling causing high biogenic productivity (Hay and Brock, 1992; Ten Haven et al., 1990; Berger et al., 1998; James and Bone, 2000, Henchiri, 2007). The precipitation of silica minerals reduces porosity as they precipitate as cement in pores (Maliva and Dickson, 1992; Chaika and Dvorkin, 2000), but early precipitation can also result in hardening of the chalk, making it resistant towards compaction and hence preserve porosity (Aase et al., 2001). Early silica diagenesis and decomposition of organic matter by microbes can also result in the formation of flint layers

(Clayton, 1986, Zijlstra, 1987, Madsen and Stemmerik, submitted). Flint layers commonly have low porosity and permeability and can thus act as barriers for oil migration.

This report focuses on the petrography of flint nodules, silicates in chalk and their distribution in the Upper Tor Member and lower Ekofisk Formation in the Ekofisk Field in order to better understand the silica diagenesis and how these levels can be distinguished by geophysical logs.

2. Geological setting

The Ekofisk Field is located in the Norwegian Central Graben, Block 2/4, southwest of the Norwegian coast (Fig. 1). The Central Graben has been divided into 17 zones based on the response of the basement to the different tectonic episodes (Gowers and Saeboe, 1985). The Ekofisk Field is together with West Ekofisk and Albuskjell Fields located north of Feda Graben in a complex faulted block (Fig. 2). The sedimentological and structural history of these fields differs much from the Eldfisk Field and other chalk reservoirs to the south.

The Central Graben was initiated by major rifting in Triassic. During the mid Jurassic, doming of the area resulted in erosion of the Triassic and Lower Jurassic sediments. Extension of the crust continued during Late Jurassic and Early Cretaceous. In the mid-Cretaceous widespread subsidence started and continued in the Late Cretaceous and Tertiary. The graben was narrow, deep and bounded by shallow platforms to the east and west. From the Late Maastrichtian to the Early Danian the platforms and structural elements inside the graben were subjected to tectonic pulses, resulting in seafloor instability and deposition of allochthonous chalk including debris flows, turbidites and mud-flow sediments in the Ekofisk area (Kennedy, 1987). Because of the northwest oriented Lindesnes ridge southwest of the Ekofisk Field, the area became depocenter for the allochtonous chalk. The seafloor topography was modest and deposition of the allochtonous chalk occurred in outer shelf or shelf slope environments at water depths of 150 to 600 m (D´Heur, 1980, Hancock, 1975; Distefano, 1980, Bramwell et al., 1999). Bottom currents were active in this environment as indicated by an east-west trending channel-like feature in the Upper Tor Member in the south western part of the Ekofisk Field (Bramwell et al., 1999). Channel systems have also been reported from the Danish North Sea where they were interpreted to have formed by south-east directed bottom currents (Esmerode et al., 2008).

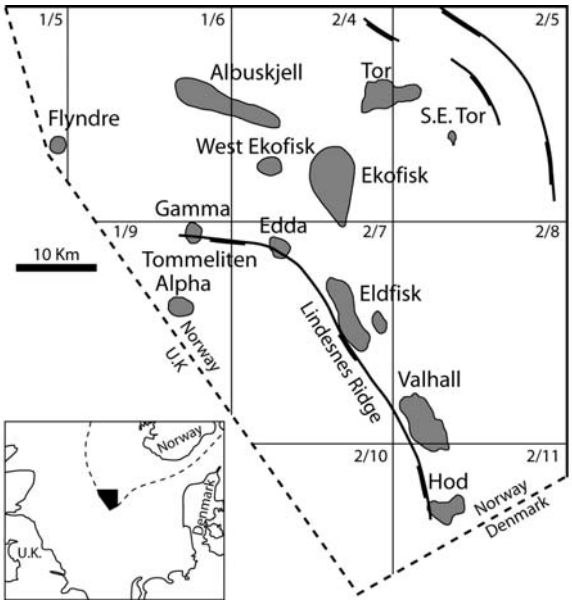

Figure 1. Map of the Norwegian North Sea with fields and faults (revised from Michaud, 1987).

The structural trap for oil and gas in the Ekofisk Field was initiated by halokinesis of the Permian Zechstein salt associated with the Central Graben extensional system that continued to early Miocene (Pekot and Gersib, 1987). The salt movement was differential and continued across the structure during Late Cretaceous and Early Paleocene time which probably caused localized variations of facies during chalk deposition.

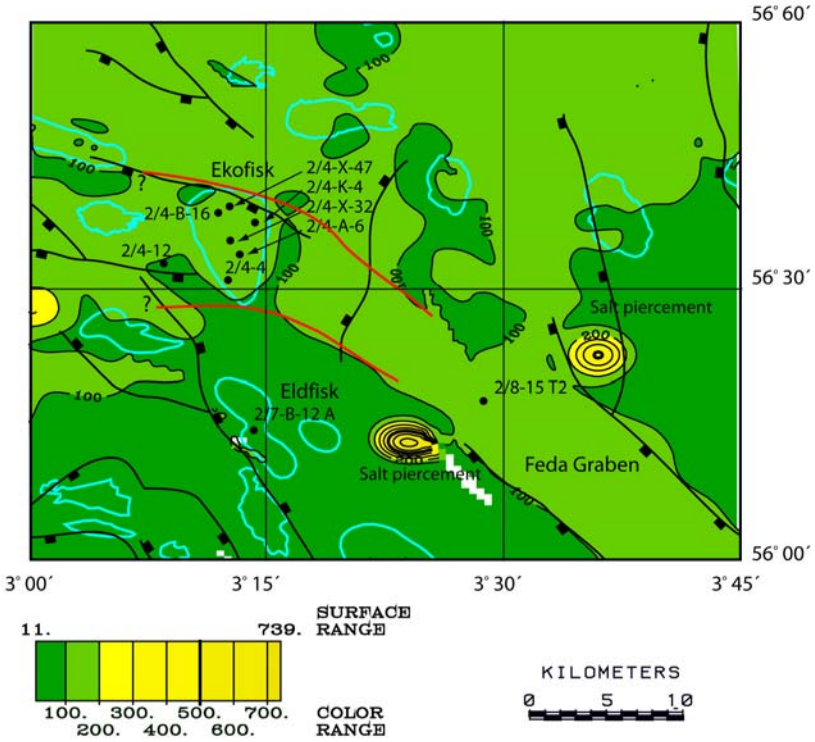

Figure 2. Isochore map of the Greater Ekofisk area and Feda Graben with location of examined wells intersecting the EE and ED Zones. Blue lines mark individual fields and red lines mark the interpreted location of a channel.

3. Materials and Methods

The 2/4-A-6, 2/4-K-4, 2/4-X-32 and 2/4-X-47 cores were chosen for this study. They form a north-south transect across the Ekofisk Field structure and the recovery and preservation of the cores are reasonable. The 2/4-X-32 and 2/4-X-47 cores are located at Reslab, Sandnes, Norway and were sampled by the author, whereas the 2/4-A-6 and 2/4-K-4 cores are located in Bartlesville, USA and were sampled following the authors instructions. Chalk samples were taken from the top of the Upper Tor Member (TA) and the lower Ekofisk Formation (EE and ED Zones). Mineralogical composition of the insoluble residue was determined on 116 samples (Appendix A). Thin sections of six flint nodules were prepared for petrography from the ED zone in the 2/4-X-47 core and of five flint nodules from the EE Zone in the 2/4-X-32 core. Lithological logs were generated on the basis of core photos and give the overall distribution of flint, marl and larger structures in the chalk.

For analysing the insoluble residue, samples were crushed in a porcelain mortar until it passed a 2 mm sieve and then cleansed for oil by Soxhlet cleaning in toluene and methanol. When the samples were dry, calcite was removed using a buffered acetic acid at pH 4.5. This mild dissolution of the calcite was used to avoid dissolution of non-calcite minerals. The X-ray diffraction (XRD) analyses of the insoluble residue were carried out on randomly oriented specimens using a Philips

1050 goniometer with Co-Kα radiation (pulse-high selection and Fe-filter). The amount of quartz in the insoluble residue was determined using 99.99% pure quartz with grain size of 4.5–45 µm as a standard. Other minerals were qualitatively determined by comparing them with standards in the software PW 1877 Automated Powder Diffraction Version 3.6j.

SEM analyses were carried out on small samples of chalk and insoluble residue which were applied on carbon tape on aluminium stubs. The samples were coated with gold in vacuum at 25 kV and 20 mA for 2–3 minutes using a SEM Coating Unit E5000. A PHILIPS XL 40 SEM equipped with a ThermoNoran energy dispersive X-ray detection system (EDX) was used for photography and qualitative chemical analysis. The petrophysical logs were supplied by ConocoPhillips, Norway.

4. Results

4.1 Lithology and stratigraphy in the Ekofisk Field

The Ekofisk Field produces from the Upper Cretaceous and Paleocene, Tor and Ekofisk Formations. The Tor Formation is subdivided into three members. The Lower Tor Member (TC) of early Maastrichtian, the Middle Tor Member (TB) and the Upper Tor Member (TA) of late Maastrichtian age. The Tor Formation is overlain by the Ekofisk Formation which is subdivided into five members. The lower Danian Ekofisk Tight Zone (EE), Reworked Maastrichtian Zone (ED), Reworked Danian Zone (EC), Tommeliten Tight Zone (EB) and the Upper Porous Zone (EA). This study focuses on the TA, EE and ED zones.

The upper 25 feet of the TA member in the 2/4-A-6 core consist of a chalk which appears brownish and contain hairlines, joints and chalk clasts in a few levels (Figs. 3, 4a). The chalk is pure and consists of 96–99% carbonate, where the insoluble residue primarily is quartz and kaolinite with minor amounts of flouroapatite, dolomite, pyrite, barite and smectite-illite (Fig. 3, Appendix A).

The Tor Formation is overlain by the Ekofisk Tight Zone (EE) of the Ekofisk Formation with thickness varying between 52–78 ft in the 2/4-X-47, 2/4-K-4, 2/4-X-32 and 2/4-A-6 wells (Fig. 3, Appendix B). The EE Zone consists mainly of bioturbated pelagic chalk with intercalated marls and flint layers and nodules (Figs. 3, 4b). Thin turbidites, debris flows and occasionally conglomerates, hard grounds and pyrite nodules do also occur. In the lower part distinct flint and marl layers can be correlated between the 2/4-K-4 and 2/4-X-32 cores, whereas no flint is present in the lower part of the EE Zone in 2/4-A-6, indicating an uneven distribution of flint in the Ekofisk Field. In the upper part of the EE Zone, flint nodules are present in the 2/4-A-6 and 2/4-K-4 cores. Additionally, flint has also been observed in the EE Zone of the 2/4-B-12 and 2/4-B-16 cores.

The EE Zone is characterized by high content of quartz and kaolinite, locally up to 50%, with subordinate smectite-illite, flouroapatite, crandelite, dolomite, barite and pyrite adding up to 70% of the bulk rock volume in some levels (Fig. 3, Appendix A). The insoluble residue is highest in the lower, flint-bearing part of the EE Zone in 2/4-K-4 and 2/4-X-32 whereas the bottom part of EE Zone in the 2/4-A-6 core where no flint is present contains less insoluble residue. The XRD and GR logs indicate a general increase in the clay content in the lower part of the EE Zone from the well 2/4-X-47 in the north to the well 2/4-A-6 in the south.

The Reworked Maastrichtian Zone (ED) consists of debris flows and slumped debris flows that contain both chalk and flint clasts (Figs. 3, 4c). Few flint layers have been observed in the 2/4-X-47. The angular flint clasts are randomly oriented and distributed whereas the flint layers are oriented

parallel with lamination in the chalk. Stylolites and joints are observed in the lower part of ED in the 2/4 K-4 and 2/4 A-6 cores. The chalk is pure with carbonate content ranging from 95–99%. The mineralogy of the insoluble residue is similar to that of the Maastrichtian TA Zone in 2/4-A-6. However, calcian albite is also present in amounts up to 1% in the ED Zone (Fig. 3, Appendix A).

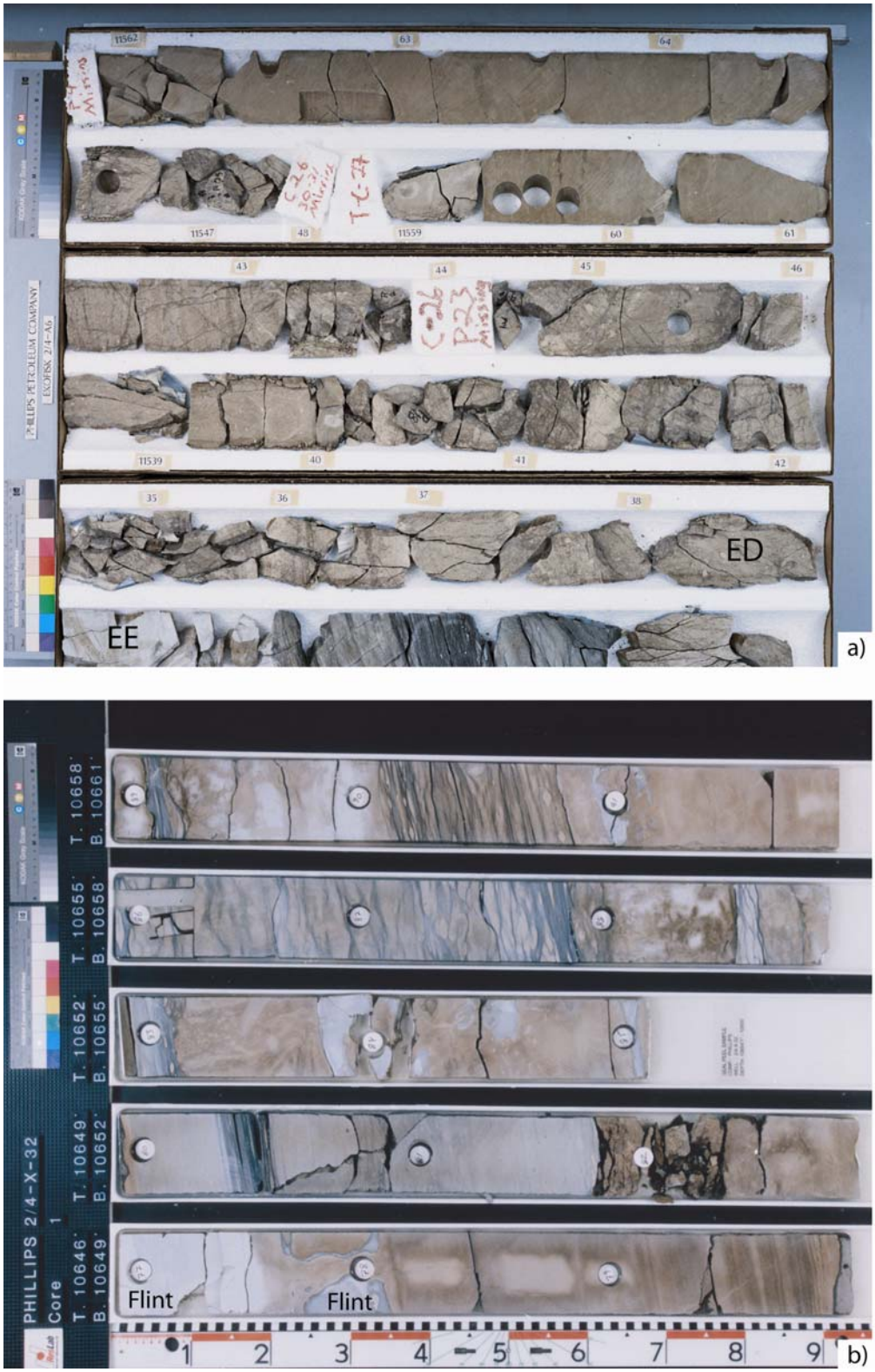

Figur 4. Core photos of a) 11531–11562 ft in 2/4-A-6 with EE and ED Zones marked, b) 10646–10661 ft in 2/4-X-32.

Figure 4 continued. c) 15781–15796 ft in 2/4-X-47 cores.

4.2 Petrography

4.2.1 Flint

4.2.1.1 EE zone

In the EE zone in 2/4-X-32, the flint forms layers of up to 30 cm that commonly are white to grey and occasionally dark (Fig. 4b). In thin section the flint is occasionally composed of zones with variable degrees of silicification, where the dark and brownish areas are the least silicified (Fig. 5a). The boundary between these zones is often abrupt and irregular.

The matrix is fine-grained and consists of microquartz and variable amounts of fossil fragments. Calcispheres and foraminifers are common whereas inoceramids and brachiopods are rare in these nodules. The fossils have been variably silicified by lutecite (variant of chalcedony), least in partial silicified patches in the flint nodules, replacing the primary calcite texture though without preserving any fine details. Moulds after sponge spicules are mostly filled by an undistinguished opaque phase but also by spherulitic chalcedony which radiates from several points (Figs. 5b and c). The spicules have a preferred orientation, which reflect sedimentary bedding. The chalk ooze has been replaced by microquartz which is the most common silica mineral in the flint nodules (Figs. 5a, b and c). Microquartz is microcrystalline with a diameter less than 20 μm and displays an equigranular texture with a pin-point extinction pattern. Oval and oblong shaped patches of coarse material consisting of carbonate fragments, calcispheres, foraminifers, dolomite and pyrite occur in the fine-grained matrix in a few flint nodules (Fig. 5d).

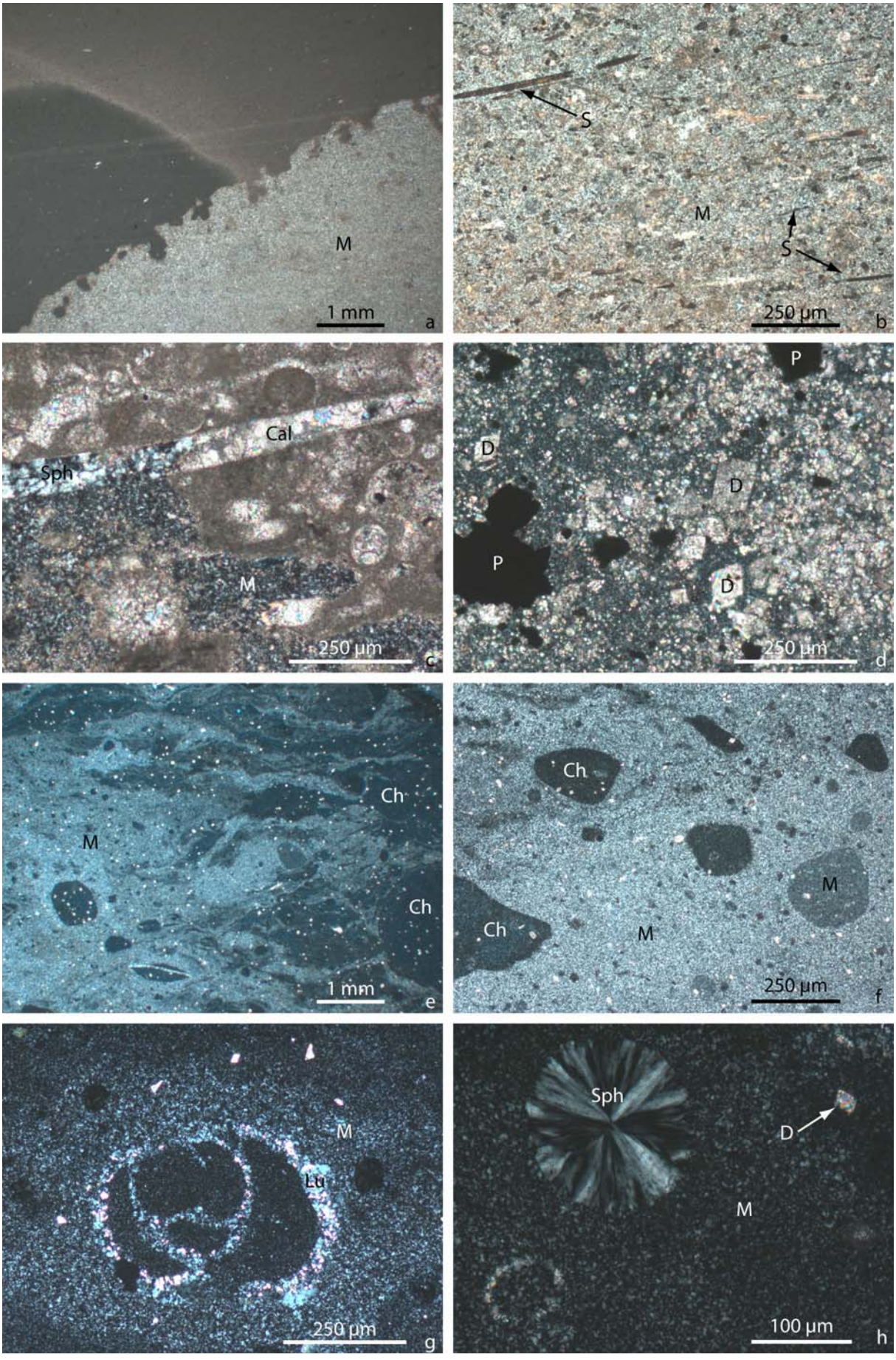
M
1 mm
a
S
M
S
250 µm
b
Cal
Sph
M
250 µm
c
P
D
D
P
D
250 µm
d
Ch
M
Ch
1 mm
e
Ch
M
Ch
M
250 µm
f
M
Lu
250 µm
g
Sph
D
M
100 µm
h

Figure 5 previous page. Micro-photographs of flint nodules from the EE Zone (a–d) and ED Zone (e–h). a) Flint nodule showing zones with varying degree of silicification by micro quartz (M). b) Nodule containing abundant imprints from siliceous spicules. c) Rind of the nodule from the previous micro-photograph with a spicule partial filled by spherulitic chalcedony (Sph) and calcite (Cal). d) Coarse-grained patch containing carbonate fragments, dolomite (D) and pyrite (P). e) Flint nodule with wavy lamination and unaltered chalk clasts (Ch). f) Unaltered and variable silicified chalk clasts. g) Foraminifer replaced by lutecite (Lu). h) Spherulitic chalcedony in frustule.

4.2.1.2 ED zone

The flint in the ED zone of the 2/4-X-47 core primarily occurs as white, greyish to dark nodules, with an angular to round shape and usually a few millimetres to few centimetres across, but layers up to 10 cm thick have been observed (Fig. 4c). All the examined flint nodules contain reworked clasts and have a wavy lamination. The clasts are sub-angular to round, up to 2 mm, and consist of unaltered chalk, partial silicified chalk or fully developed flint (Figs. 5e and f). The wavy lamination is defined by partially silicified chalk layers in the flint (Fig. 5e).

Foraminifers, inoceramids, brachiopods and calcispheres are common in the flint nodules, where lutecite replaces the shells (Fig. 5g). Microquartz is the most common phase and has replaced the chalk ooze (Figs. 5a–h). Spherulitic chalcedony is less common and occurs as void-filling cement in frustules (Fig. 5h). Dolomite is common in the nodules as up to 50 μm rhombohedral crystals (Fig. 5e–h).

4.2.2 Chalk and marl

The mineralogy of the insoluble residue of the chalk and marl was determined by XRD and confirmed by SEM and EDX. The analyses indicate the presence of quartz, kaolinite, smectite-illite, calcian albite, fluor-apatite, crandelite, dolomite, pyrite and barite (Fig. 3, Appendix A). The SEM analyses show that the mineralogy and morphology of the insoluble residue are almost identical in all the zones and cores. The insoluble minerals are therefore described in general.

Quartz is the most common phase in the insoluble residue and occurs both as single crystals and aggregates. The crystals are six-sided and single or double terminated by six-faced pyramids and can be up to 5 μm long (Fig. 6a). The aggregates are often less than 1 μm but can reach 5 μm (Fig. 6b). They are comprised of sub-micron sized quartz crystals with a similar crystal habit as the single crystals. Both crystals and aggregates are commonly associated with kaolinite and more rarely with smectite-illite (Fig. 6a).

Kaolinite occurs in all samples but is most common in the marl layers. It occurs as hexagonal shaped crystals arranged in booklets, commonly 5 μm in diameter (Fig. 6c). The kaolinite is present both in voids and in the matrix (Fig. 6c, d). The kaolinite is, as mentioned above, often associated with quartz aggregates and quartz crystals (Fig. 6a). EDX analyses indicate that kaolinite primarily contains Si, Al and O but often also traces of Ca.

Smectite-illite was present in trace amounts in all samples analysed by XRD. The presence was confirmed by SEM analyses which indicate a flaky and delicate morphology. In one sample from the ED Zone in 2/4 X-47 it forms a spherical aggregate, 40 μm in diameter, inside a foraminifer chamber (Fig. 6e). This aggregate consists of flaky smectite-illite and minor amounts of sub-micron sized quartz aggregates (Fig. 6f). In the adjacent foraminifer chamber flaky smectite-illite occurs together with a single euhedral quartz crystal. Chemically the smectite-illite consists primarily of Si, Al, O, minor amounts of Ca and occasionally small amounts of K and Mg.

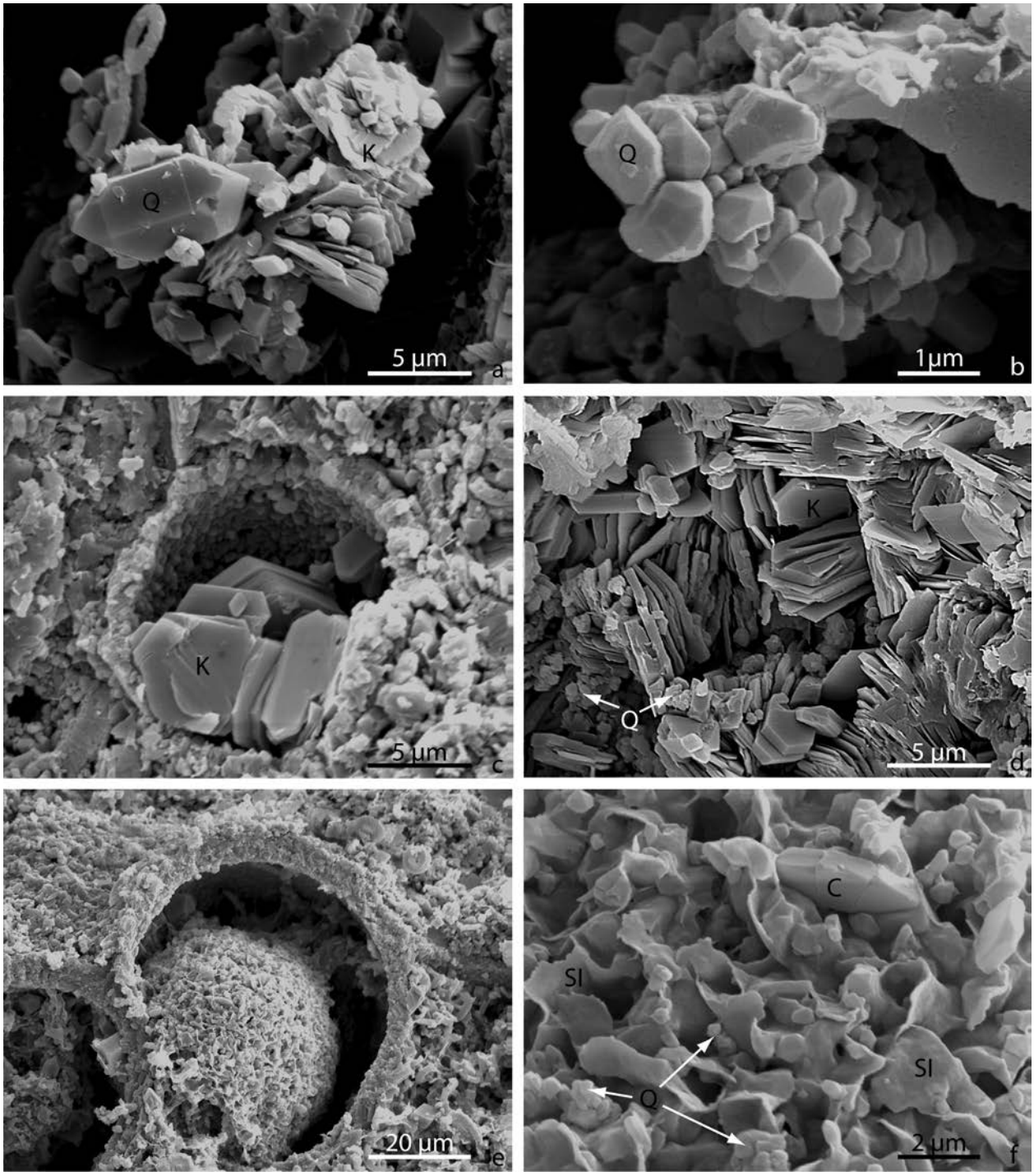

Figure 6. SEM images a) Single quarts crystal (Q) sitting on Kaolinite (K) b) Quartz aggregate consisting of sub-micron sized quartz crystals c) Kaolinite inside a calsisphere d) Kaolinite in matrix e) Spherical aggregate of smectite-illite inside a foraminiferal chamber f) Close up on the spherical aggregate showing a flaky and delicate structure of smectite-illite (SI), and the presence of sub-micron sized quartz crystals and coccolith fragments (C.)

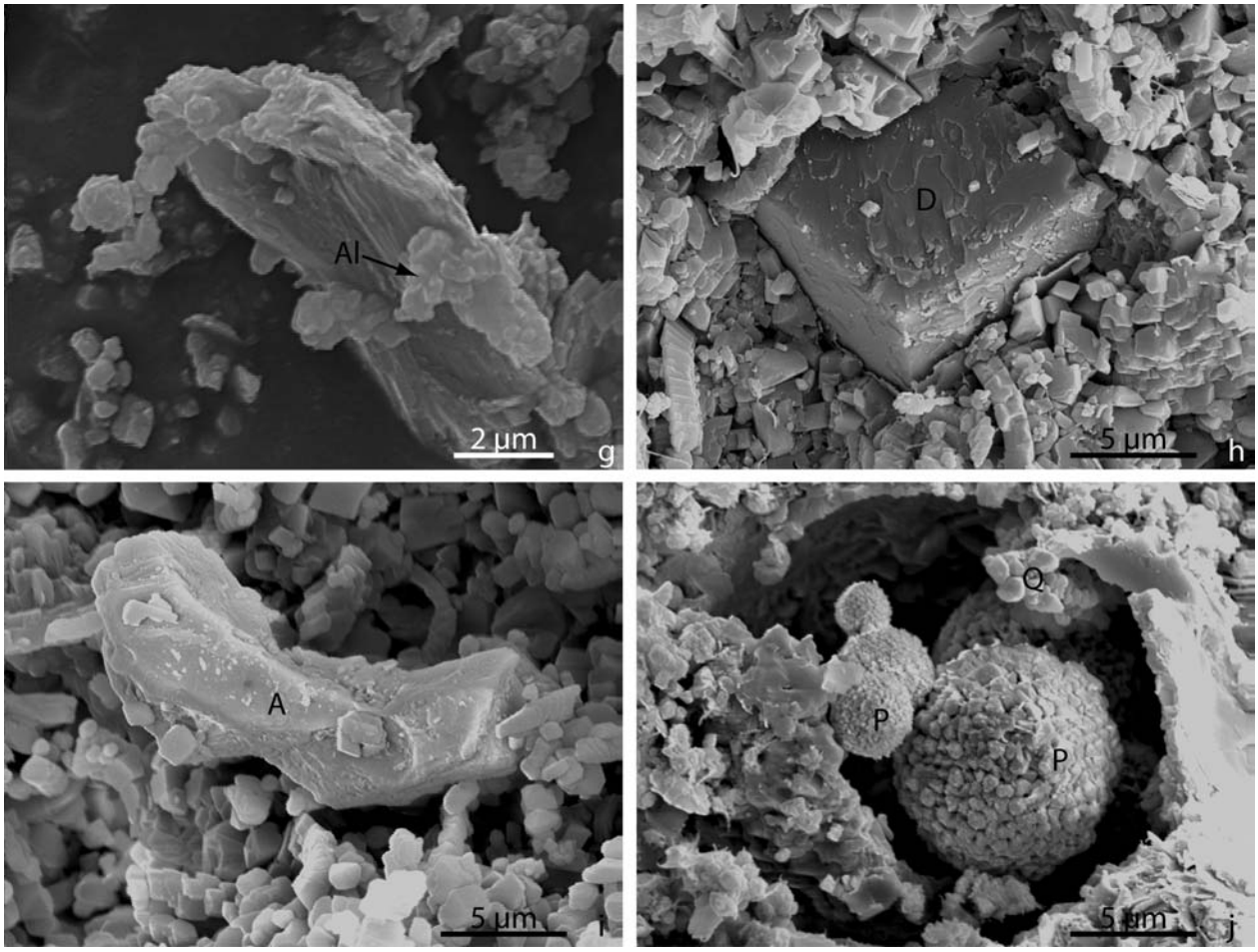

Figure 6 continued. *g) Albite (Al) aggregate in insoluble residue h) Dolomite rhombohedra in the chalk matrix i) Subhedral grain of flour-apatite (A) j) Spherical pyrite (P) and quartz aggregates inside a calcispheres.*

Calcian albite is present primarily in the ED Zone in the 2/4 X-47 core, in amounts of less than 1% as indicated in the XRD analyses (Appendix A). The plagioclase occurs as sub-micron sized aggregates that consist of small crystallites (Fig. 6g). It chemically consists of Si, Al, O, Na and Ca.

The occurrence of dolomite is highly variable, as it is not present in all samples, but comprises up to 13% in some chalk and marl layers in the EE Zone. In the TA and ED zone it comprises less than 2%. The dolomite is rhombehedral and the edges are up to 10 µm long (Fig. 6h). The dolomite seems to occur in the matrix where coccolith fragments occasionally are incorporated in the crystals or have left marks on their surfaces. EDX shows that the dolomite contains Ca, Mg and also minor amounts of Fe, indicating a ferroan dolomite; this is also supported by a DTA analysis.

Phosphates as fluor-apatite and crandelite ($CaAl_3(PO_4)_{1.5}(OH)\cdot 5H_2O$) are present in the chalk. Fluor-apatite occurs in all samples and comprises 0.2–0.3% in the ED and TA Zones and up to 2.6% in the EE Zone. Fluor-apatite has been difficult to find in the SEM and only a single large subhedral grain has been recorded (fig. 6i). The majority of the fluor-apatite is probably present as nano-sized particles, below the resolution of the instrument. Crandelite only occurs in a few samples and has not been identified by SEM in this study.

Pyrite occurs in most of the chalk samples in amounts from 0.1–0.2% and up to 1%, whereas it comprises 2–6% in some marls. It has been observed in calcispheres where it occurs as spherical aggregates of sub-micron sized crystallites (Fig. 6j). Barite occurs in trace amounts in a few samples but the morphology and relations have not been established.

4.3 Effects of flint and insoluble minerals in chalk on the geophysical log respond

To determine the effects of flint and insoluble residue in the chalk on the geophysical log response their relation have been tested. The test was carried out in the flint bearing EE and ED Zones by applying different cross plots. The GR log reflects the presence of marly layers well and was used to establish the relation between core and log depth. It was necessary to shift the cores 23, 3 and 19 ft in the ED and EE Zones of the wells 2/4-K-4, 2/4-X-32 and 2/4-A-6 respectively. This enables a comparison between the petrophysical logs and the flint, marl and the insoluble residue in the cores.

Flint consists of almost massive SiO_2 and has low porosity and high density compared to the chalk. Therefore the NPHI and RHOB logs were found to be the best indicators of the presence of flint as illustrated with data from the 2/4-X-32 well (Fig. 3, 7a). Two of the three flint layers in the bottom part of this core plots on the sandstone trend whereas the third almost plots on the limestone trend. The low estimated porosity and high density of flint compared to the chalk is especially clear in the 2/4-X-47 well (Fig. 7b).

Marl layers plot between the limestone and dolomite trends, as a result of the presence of abundant kaolinite (Fig. 7a). The marls are characterized by high gamma readings, high RHOB and low NPHI, with porosity generally lower than the pure chalk and some as low as the flint.

The effects of quartz and kaolinite on the petrophysical logs are significant when comparing the EE Zone with the TA and ED Zones (Fig. 3). The EE Zone has higher response from the GR and RHOB whereas the NPHI is lower. Further, levels with high quartz content e.g. in the lower part of 2/4-A-6 can be distinguished by high density and low porosity comparable to that of the flint layers in the other wells.

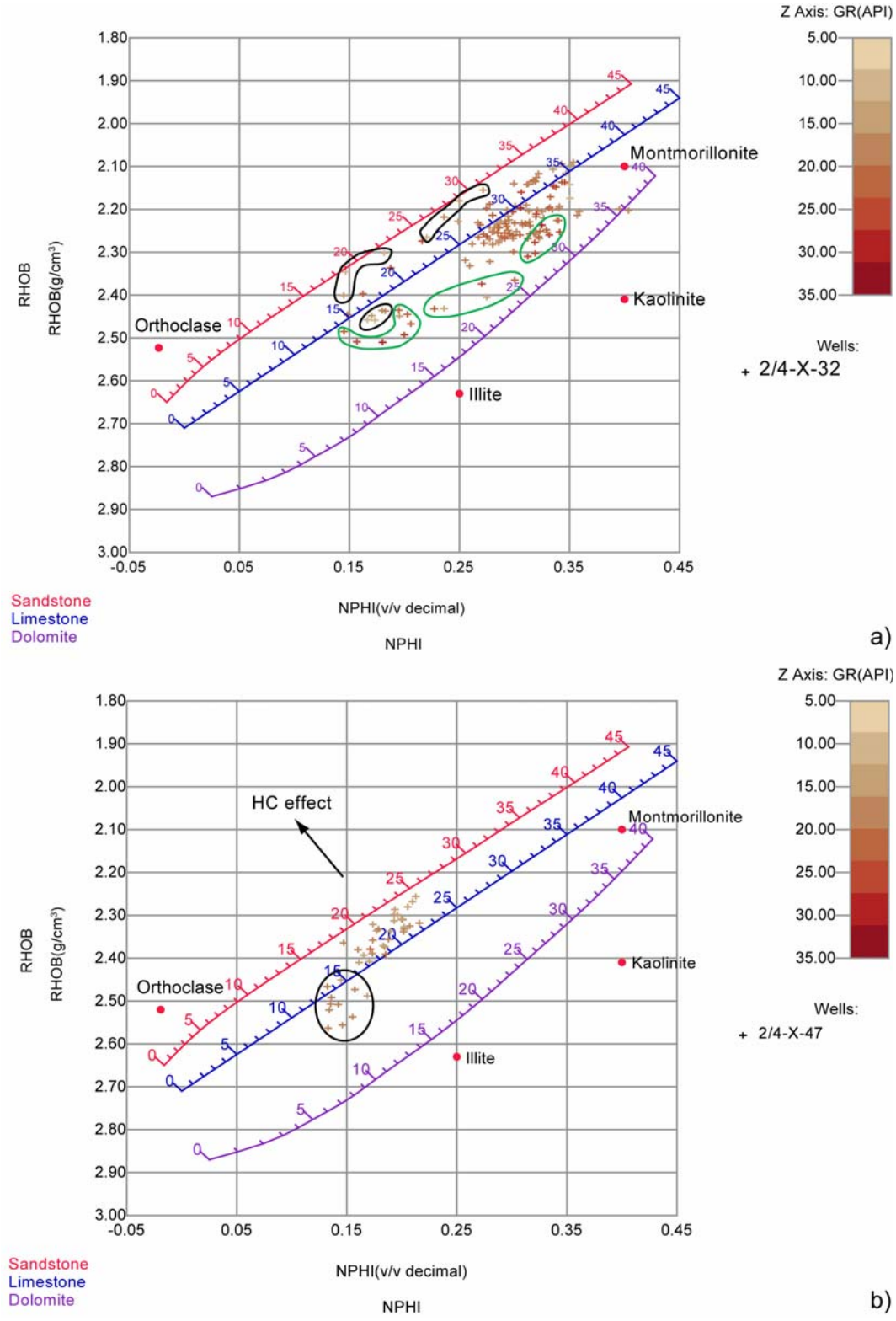

Figure 7. NPHI-RHOB cross plots where GR is illustrated by the colour scale. a) Three flint layers (black lines) and three marl layers (green lines) can be identified in EE Zone in the well 2/4-X-32. Both flints and marls generally have higher density and lower porosity than chalk. No hydrocarbons effect on data was present in this interval. b) Clear density and porosity contrasts between flint and chalk in cross plot from the ED Zone in the well 2/4-X-47. Note that data is affected by hydrocarbons in this plot.

5. Discussion

Both early sea-floor related and late burial silica diagenesis have occurred in the form of flint formation and late mineral reactions in the Tor and Ekofisk Formations in the Ekofisk Field. It is important to understand the diagenetic processes when predicting distribution of diagenetic precipitates as it will improve prediction of reservoir quality.

5.1 Early diagenetic precipitation of flint

5.1.1 Silica source

From the petrographic examination it is clear that the flint is composed of almost pure quartz in the form of microquartz, chalcedony and lutecite. The occurrences of fossils inside the flint nodules indicate that silica replaced chalk. The source for silica is interpreted to have been biogenic, as abundant moulds and imprint after siliceous sponge spicules were found in some of the flint nodules. This indicates that sponge colonies contributed with silica to the formation of flint in the Ekofisk Formation in the Ekofisk Field. A biogenic silica source for flint is widely accepted and has been argued for by several authors e.g. Wise and Weaver (1974), Clayton (1986), Zijlstra (1987) and DeMaster (2004).

5.1.2 The flint forming processes

5.1.2.1 The driving mechanisms for initial mobilisation of silica

The processes involved in the dissolution of the biogenic silica and replacement of the chalk by flint are not clear in the EE Zone because of the limited lateral information in the cores. The processes are further complicated by the presence of terrigenous material, especially clay. Clay minerals decrease the solubility of silica and hence inhibit the initial flint forming stages, making the processes less obvious (Iler, 1973; Dixit, 2001, Brickmore, 2006). In the time equivalent Stevns-1 and 2 cores, eastern Denmark, flint nodules and layers are observed to form during periods of none or low deposition around 0.5 m below the sea floor (Madsen and Stemmerik, submitted).

The presence of abundant dolomite in some levels in the chalk in the Ekofisk Field infers that microbial activity has played a role during early diagenesis, similar to what is proposed for the flint in the Stevns-1 core. The involvement of microbes in the formation of flint has also been suggested by previous studies (Clayton, 1986; Zijlstra, 1987). The formation of flint and dolomite is related to several aerobic, subaerobic and anaerobic microbial processes which occur in specific zones in the sediment (e.g. Kristensen, 2000) (Fig. 8a). The dolomite precipitates in the reduced zone where the kinetic inhibitors for dolomite precipitation, as high hydration energy of Mg^{2+}, low CO_3^{2-} activity and SO_4^{2-} is overcome by the anaerobic microbial processes (Fig. 8b) (Vasconcelos et al., 1995; Vasconcelos and McKenzie, 1997; Wright, 2000; Wright and Wacey, 2005).

At the redox boundary a group of sulphide oxidizing bacteria, *Beggiatoa* and *Thiovulum* ssp., nourish themselves by oxidizing the sulphides and hydrides produced in the reduced sediment (Eq. 1) (Brune et al. 2000; Kristensen, 2000).

$$HS^- + 2O_2 \rightarrow SO_4^{2-} + H^+ \qquad \text{Eq. 1}$$

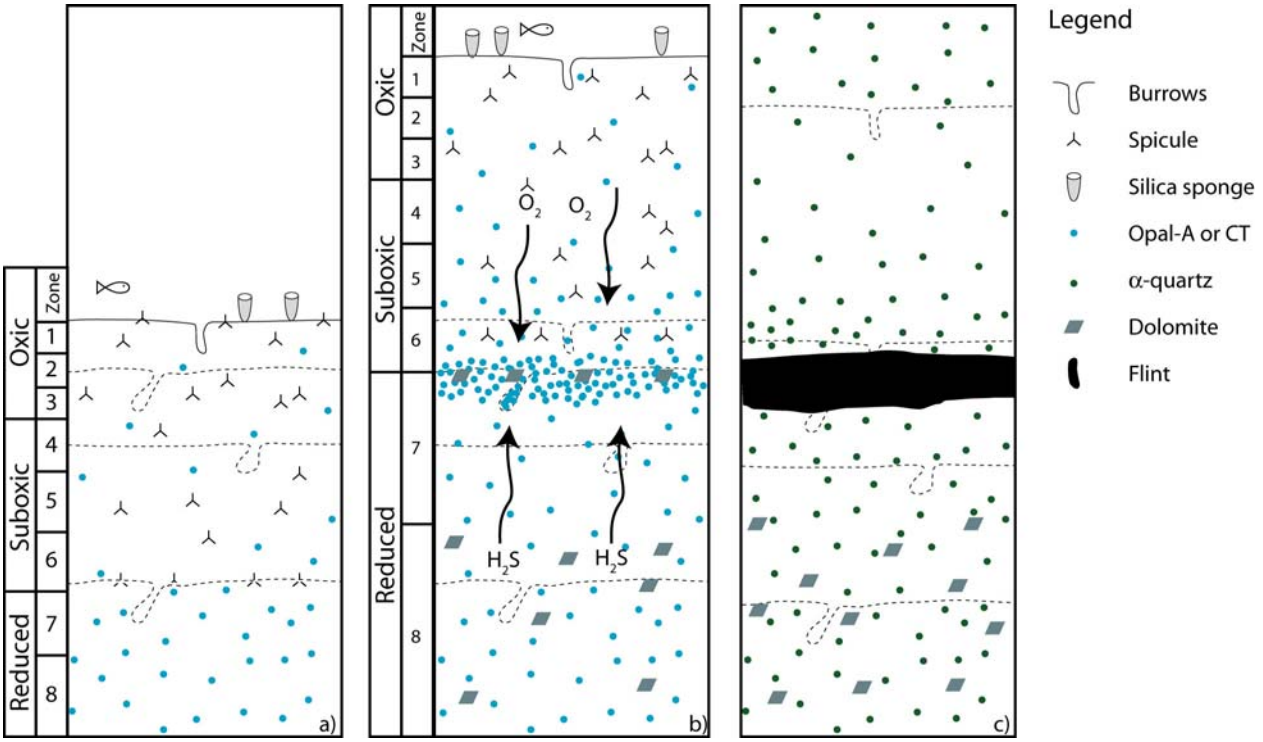

Figure 8. Model of flint formation. a) Continuous sedimentation result in even distribution of opal-A or -CT aggregates. b) Sedimentation stops and oxic, suboxic and reduced sediment along with bacteriological metabolic zones remain at the same level for a longer period of time. Metabolic zones: 1) aerobic respiration, 2) nitrification, 3) sulphide oxidation, 4) manganese oxide reduction, 5) denitrification, 6) iron oxide reduction, 7) sulphate reduction and 8) methanogenesis. At the redox boundary, between the suboxic and reduced sediment, sulphide oxidizing bacteria oxidizes sulphides, resulting in production of H^+, dissolution of carbonates and liberation of hydroxyl complexes. The hydroxyl complexes act as catalysts for silica precipitation forming silica gel or opal-CT. The silica is interpreted as being derived from siliceous sponge spicules in the upper part of the sediment. Simultaneously with the silicification at the redox boundary dolomite precipitates in the reduced sediment. c) Sedimentation resumes and the metabolic zones move upward ending precipitation of silica at a specific level. During burial diagenesis opal-A and -CT are converted to α-quartz.

Much energy is released in this process which liberates hydrogen ions creating an environment of low pH at the redox boundary (Jørgensen, 1982; Brune et al. 2000; Kristensen, 2000). This environment is interpreted to initiate the flint forming process and will be discussed below. These sulphide oxidizing bacteria live at the redox boundary in a narrow zone (Jørgensen and Revsbech, 1983; Fenchel and Bernard, 1995; Fenchel and Glud, 1998), which also can explain why flint is restricted to narrow horizons.

The initial flint forming processes occurred during periods of non-deposition or low sedimentation, which fixed the redox boundary at a specific depth. Oxidation of hydrides by sulphide oxidizing bacteria living at the redox boundary is interpreted to have caused the initial precipitation of silica-gel or opal-CT. Silica was sourced from biogenic opal-A which dissolved in the upper oxic part of the sediment (Fig. 8b).

5.1.2.2 Replacement process

The petrographic observations clearly indicate that the flint in the Ekofisk Field is the result of replacement and cementation of chalk by silica, primarily microquartz and lutecite. This process was evidently accompanied by the precipitation of dolomite.

The flint forming process initiated in an acidic environment created by the sulphide oxidizing bacteria at the redox boundary (Fig. 8b). Carbonates dissolved in this environment, causing the liberation of positively charged hydroxyl complexes such as $Mg(OH)_2$. These hydroxyl complexes flocculate dissolved $Si(OH)_4$ from siliceous sponge, resulting in the liberation of water and formation of a $Si(OH)_2$ hydroxyl complex (Williams and Crerar, 1985) (Eq. 2). The $Si(OH)_2$ hydroxyl complex then reacts with a new $Si(OH)_4$ molecule, forming a new hydroxyl complex. This process can be repeated numerous times and in theory form long chains of silica, resulting in the formation of silica gels or opal-CT. The dissolution of the chalk resulted in high CO_3^{2-} activity and high concentration of Mg^{2+} which caused simultaneous precipitation of dolomite and silica.

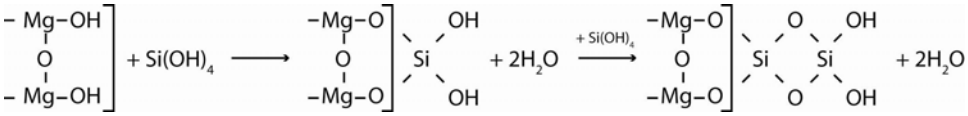

Eq. 2

5.1.2.3 Phase transformations

During burial the silica gel or opal-CT are transformed to more ordered and stable silica phases. Phase transformations from biogenic opal-A to opal-CT to α-quartz are well documented in the Ocean Drilling Project (ODP) and the Deep Sea Drilling Project (DSDP) cores (von Rad and Rösch, 1974; Wise and Weaver, 1974; Keene, 1975; Kastner, 1981). The opal-CT bearing porcellanites dominate in the youngest sediments whereas flint composed of α-quartz is limited to the older parts of the drilled successions. It is likely that the same phase transformations took place in the flint layers from the EE and ED Zones in the Ekofisk Field, which is now composed of α-quartz in the form of microquartz, chalcedony and lutecite (Fig. 8c).

5.1.3 Distribution of flint

Flint occurs in all the studied cores from the field although well 2/4-A-6 in the south did not intersect any flint in the lower part of the EE Zone. The 2/4-A-6 core has levels with high quartz content and the geophysical log response is similar to that seen in the sections containing flint. These levels are interpreted to be laterally less silicified extensions of the flint layers. Lateral variations in microbial decomposition of organic matter and the presence of silica, is interpreted to have caused this unevenly distribution of flint in the field.

Siliceous sponges are most likely the silica source, and abundant spicules in some flint nodules in the EE Zone indicate that sponge colonies probably had a controlling factor on where flint formed. Siliceous sponges are known to thrive in bottom currents rich in nutrients, particulate matter and dissolved silica. Detailed study of recent framework siliceous sponge reefs on Western Canadian Continental Shelf show that these sponge reefs are generally restricted to channels (Austin, 1998; Conway et al., 2005; Whitney et al., 2005).

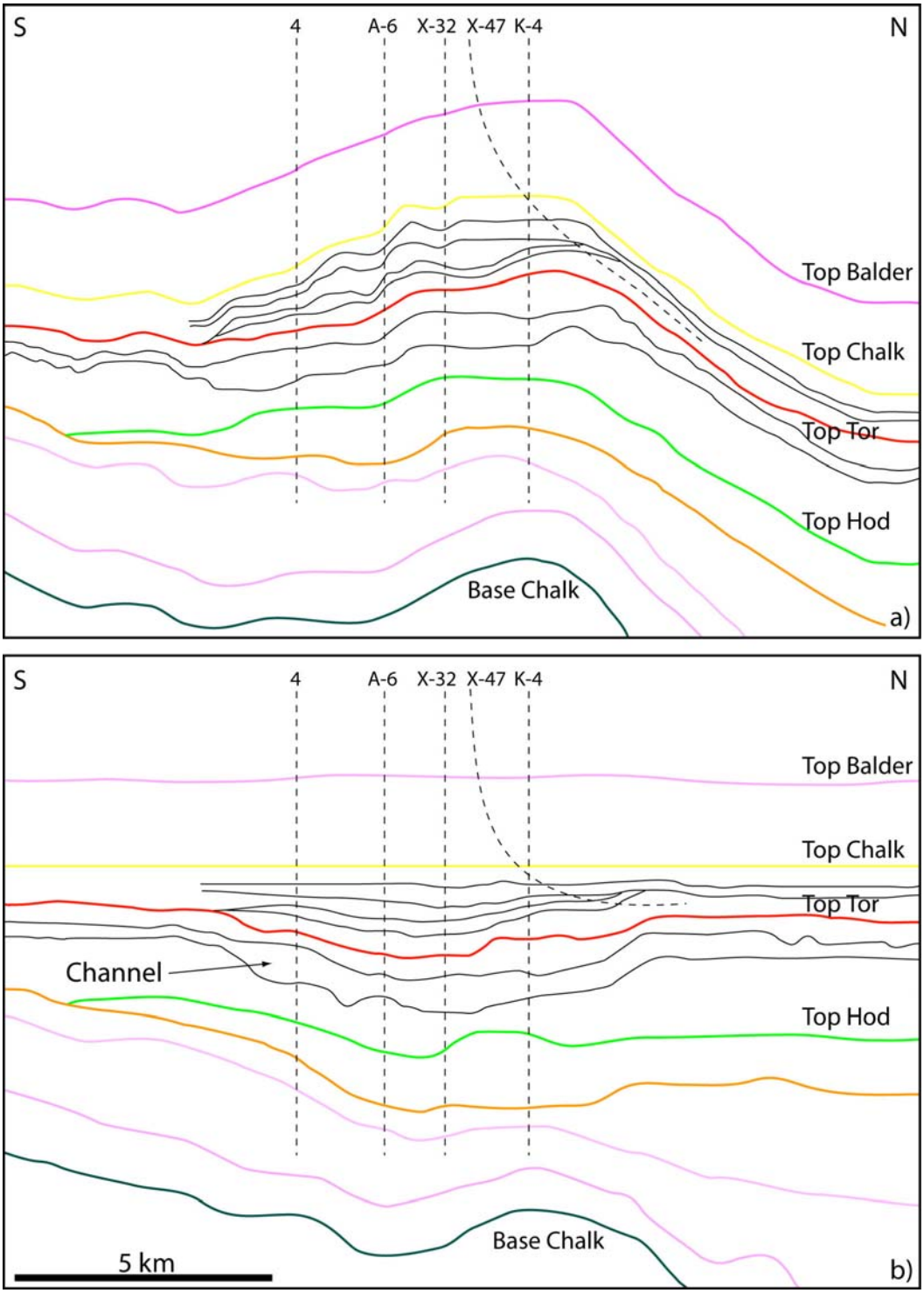

Figure 9. Interpreted north-south seismic section and location of wells across the Ekofisk Field. b) Flattened section by using Top Chalk as reference. Note the thickening of the Ekofisk Formation (between Top Tor and Top Chalk).

Bramwell et al., 1999 recorded an east-west trending channel in the upper Tor Formation in the Ekofisk Field which indicates bottom currents in the area. If bottom currents were active at the end of the Maastrichtian it is possible that currents also were active in the beginning of Palaeocene. Seismic sections and well data show thickening of the EE Zone and the whole Ekofisk Formation in the north-south transect across the Ekofisk Field (Figs. 3 and 9, Appendix B). The interpreted

seismic units inside the Ekofisk Formation further resemble channel geometries (Fig. 9b). This indicates that a channel system with active bottom currents probably existed in the early Palaeocene.

Thickening of the Ekofisk Formation outside the field (estimated from confidential seismic lines) reveals a possible northwest-southeast trending channel (Fig. 2). In the northwest, the channel bends slightly towards the south whereas it is focused into the Feda Graben in the southeast. The bottom currents that could have produced this channel probably had a south-eastern flow direction (Esmerode at al., 2008). However, any flow direction would have supplied sponge colonies with nutrients and dissolved silica.

In the lower part of the EE Zone, flint is most abundant in the northern part of the field, which may indicate highest nutrient and silica supply and possibly strongest bottom currents there (Fig. 10a). The EE Zone is also thickest in this area (2/4-X-32 and 2/4-K-4) which was probably caused by baffling of suspended sediment by the siliceous sponges. The unevenly distribution of flint in the EE Zone within the field can possibly be explained by helical flow in the bend of the interpreted channel system where the northern current component would be the strongest (Boggs, 2001) (Fig. 10a). This probably led to higher concentrations of silica and flint in the EE Zone in the northern part of the field.

The Maastrichtian chalk of the ED Zone was clearly reworked before the phase transformation to α-quartz occurred. This is evident from the presence of chalk and partial silicified clasts inside the flint nodules. The reworking of the Maastrichtian chalk, most likely from the Lindesnes Ridge to the south was triggered by tectonic instability in the Central Graben after the deposition of the EE Zone. This caused a random distribution of flint in the ED Zone, which can not readily be predicted. But flint in the ED Zone seems to be concentrated in the northern part of the field (Fig. 10b, Appendix B).

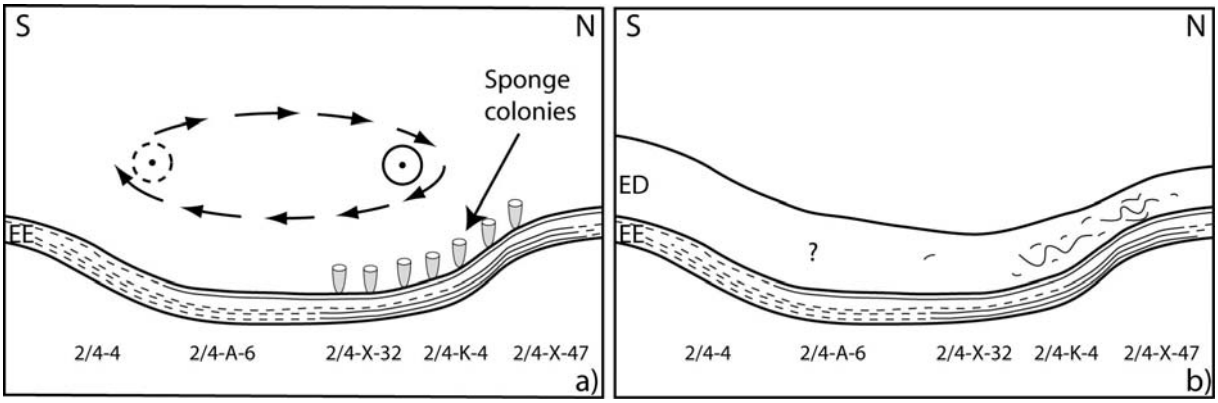

Figur 10. Interpreted palaeo setting for the deposition of EE Zone where helical flow, with a strong north current component cause sponge colonies to thrived, resulting in formation of flint layers in preferentially the northern part of the Ekofisk Field. Flint layers are marked with thin lines and silicified horizons that are correlated with flint layers are marked with thin broken lines. Arrows indicate the helical flow. The circular symbols indicate flow towards south-east and the broken one indicate lower flow rates. b) The ED Zone consists of reworked Maastrichtian chalk and flint which was probably derived from the south.

The interpreted channel system imply that the bottom currents could have controlled where the sponges lived and hence where flint formed. To test this hypothesis, additional wells were checked for the presence of flint, using core photos and logs. Well 2/4-12 west of the field and well 2/8-15-T2 in the Feda Graben, which both are located in the interpreted channel, contain flint (Fig. 2). In the southern part of the Ekofisk Field logs from well 2/4-4 do not indicate significant flint layers, but high concentrations of quartz is still present. Well 2/7-B-12A from the Eldfisk Field, which is outside the interpreted channel, does not contain any flint nodules in the Ekofisk Formation (Fig. 2). These observations support that the distribution of flint and hence their formation is likely to reflect the presence of silica sponge colonies. However, the unevenly distribution of wells makes the interpretation uncertain.

5.2 Late diagenetic mineral reactions

The authigenic silicate minerals as kaolinite, smectite, quartz and feldspars are present in the chalk and witness of later mineral reactions and phase transformations.

5.2.1 Source

The source for the authigenic clay minerals is probably smectite and feldspars which have previously been interpreted to be of terrigenous origin (Kennedy, 1987). The close association between quartz and kaolinite as seen in SEM and XRD indicates that they originated from same mineral reaction, probably from detrital smectite in the chalk. A biogenic source for kaolinite is unrealistic as the siliceous skeletons and spicules only contain 0.3–0.4% aluminium (Sandford, 2003). Huge amounts of biogenic silica would be required to form the kaolinite observed and at the same time large quantities of Si should disappear out of the system. However, biogenic opal-A from radiolarians or sponge spicules which occasionally are abundant may be an additional source for silica and may have contributed to the formation of authigenic quartz.

5.2.2 Late Diagenesis

Some of the quartz is believed to originate from phase transformations of biogenic opal-A to opal-CT and finally to quartz (Williams et al., 1985). However, the majority of the quartz is found in close association with kaolinite indicating that quartz also formed from a more complicated mineral reaction during burial. A likely reaction involves the release of silica from silicate minerals as detrital smectite. The disappearance of smectite and the formation of illite with depth are well known in the Central Graben, North Sea and other sedimentary basins and reflect depth-related diagenetic reactions (Compton, 1991; Abercrombie et al., 1994, Drits et al., 1997). However, since kaolinite is the most abundant clay mineral in the studied interval, a slightly different mineral reaction is suggested where smectite is transformed to authigenic kaolinite and little smectite-illite (Eq. 3).

smectite + K-feldspar → kaolinite + smectite-illite + quartz + dolomite Eq. 3

The fact that kaolinite is the main clay mineral precipitated, indicates that little potassium was available, as an additional potassium source, e.g. K-feldspar is needed to form illite (Hoffman and Hower, 1979, Compton, 1991). The formation of kaolinite and smectite-illite is probably the result of release of Mg and Fe from the octahedral layer in the smectite (Hower et al., 1976). During this transformation aluminium is conserved in the structure and Si is released (Compton, 1991), which

enabled precipitation of quartz near the kaolinite. Alteration of the detrital feldspars contributed with potassium to the system to from the smectite-illite. However, since kaolinite is the most abundant clay mineral the system generally must have been potassium poor.

The mineral reaction which formed the spherical smectite-illite and quartz aggregates observed in a sample from the ED Zone (Fig. 6e–f) is different from the general one (Eq. 4). It probably formed by a more simple reaction that involved same reactants but resulted in precipitation of smectite-illite and quartz (Eq. 4). This reaction could have occurred in a locally potassium-rich system (e.g. from K-feldspar) inside the foraminiferal chamber, resulting in precipitation of smectite-illite instead of kaolinite.

smectite + K-feldspar → smectite-illite + quartz Eq. 4

6. Conclusions

Both early and late diagenetic processes can be distinguished in the EE and ED Zones in the 2/4-K-4, 2/4-X-32, 2/4-A-6 and 2/4-X-47 cores in the Ekofisk Field. The precursor to flint formed during early diagenesis close to the seafloor. South-east directed bottom currents supplied water rich in nutrients, particulate matter and silica which nourished siliceous sponge colonies in especially the northern part of the Ekofisk Field. When sponges died spicules was dissolved and organic matter was decomposed by microbes initiating the flint forming process. However, only during periods with low sedimentation rates, when the redox boundary was fixed at a specific depth, flint was produced. Bacterial reduction of sulphate and oxidation of sulphides at the redox boundary by sulphide oxidizing bacteria created an acidic environment able of dissolving carbonate and liberate positively charged hydroxyl complexes that catalysed flocculation of dissolved silica, forming silica gels or opal-CT. During burial to depths of around 11000 ft, phase transformation of opal-CT to α-quartz resulted in the flint nodules and quartz particles seen in the chalk today. The chalk in the ED Zone was evidently reworked prior to the phase transformation to α-quartz.

Late mineral reactions involving dissolution of detrital smectite and K-feldspar, and precipitation of kaolinite, smectite-illite, quartz and dolomite occurred in the TA, EE and ED Zones. Preferentially kaolinite and little smectite-illite formed by addition of Al, K and release of Mg, Fe and Si from smectite. The studied intervals represent a potassium-poor system where kaolinite precipitated rather than smectite-illite. Other diagenetic non-silicate minerals as fluor-apatite, crandelite, barite and pyrite are also present.

The petrophysical logs RHOB and NPHI can successfully be used for identifying flint layers and chalk with high content of quartz and kaolinite. NPHI-RHOB cross plot indicate that the porosity has been reduced by early diagenetic flint formation and late diagenetic void filling quartz and kaolinite in the chalk.

Acknowledgements

The Ekofisk Group at ConocoPhillips, Norway is acknowledged for provided data on request and discussions. Finn Christian Jakobsen and Lars Kristensen, the Geological Survey of Denmark and Greenland (GEUS), are thanked for help with the petrophysical logs, seismic and for valuable discussions and review of the report. Per Ekelund Andersen (GEUS) loaded the provided files and assisted with technical help.

References

Aase, N.E.; Bjorkum, P.A. and Nadeau, P.H. (2001). The effect of grain-coating microquartz on preservation of reservoir porosity. Bulletin-American Association of Petroleum Geologists 80: 1654–1673.

Abercrombie, H.J.; Hutcheon, I.E.; Bloch, J.D. and Decaritat, P. (1994). Silica activity and the smectite-illite reaction. Geology 22: 539–542.

Austin, W.C. (1998). The relationship of silicate levels to the shallow water distribution of Hexactinellids in British Columbia. Mem. Queensland Mus. 44: p. 44.

Berger, W.H.; Wefer, G.; Richter, C.; Lange, C.B.; Giraudeau, J. and Hermelin, O. (1998). The Angola-Benguela upwelling system: paleoceanographicsynthesis of shipboard results from LEG 175. *in* G. Wefer, W. H. Berger, G. Richter et al, Proceedings of the Ocean Drilling Program, Initial Reports. 175: 505–531.

Boggs, S.J. (2001). Principles of sedimentary and stratigraphy. Upper Saddle River, New Jersey Prentice Hall. p. 726

Bramwell, N.P.; Caillet, G.; Meciani, L.; Judge, N.; Green, N. and Adam, P. (1999). Chalk exploration, the search for a subtle trap, *in* Fleet, A.J. and Boldy, S.A.R., Petroleum Geology of Northwestern Europe, London, England, The Geological Society, London: p. 911–937.

Brickmore, B.R.; Nagy, K.L.; Gray, Amy K. and Brinkerhoff, A. Riley (2006). The effect of $Al(OH)_4^-$ on the dissolution rate of quartz. Geochimica et Cosmochimica Acta 70: 290–305.

Brune, A.; Frenzel, P. and Cypionka, Heribert (2000). Life at the oxic-anoxic interface: microbial activities and adaptations. FEMS Microbiology Reviews 24: 691–710.

Chaika, C. and Dvorkin, J. (2000). Porosity reduction during diagenesis of diatomaceous rocks. Bulletin-American Association of Petroleum Geologists 84: 1173–1184.

Clayton, C.J. (1986). The chemical environment of flint formation in Upper Cretaceous chalk, *in* Sieveking, G.D.G., and Hart, M.B., The scientific study of flint and chert: Cambridge, Cambridge University Press: p. 43–54.

Compton, J.S. (1991). Origin and diagenesis of clay minerals in the Monterey Formation, Santa Maria Basin area, California. Clays and Clay Minerals 39: 449–466.

Conway, K.W.; Barrie, J.V. and Krautter, Manfred (2005). Geomorphology of unique reefs on the western Canadian shelf: sponge reefs mapped by multibeam bathymatry. Geo-Mar. Lett. 25: 205–213.

Demaster, D.J., (2004). The diagenesis of biogenic silica: chemical transformations occurring in the water column, seabed, and crust, *in* Holland, H.D. and, Turekian, K.K., Treatise on geochemistry, Amsterdam, Elsevier Ltd: p. 87–98.

D'Heur, M. (1980). Chalk reservoir of the West Ekofisk Field. The sedimentation of the North Sea Reservoir rocks. Oslo, Norwegian Petroleum Society.

Distefano, M.; Feazel, C.T.; Park, R.K.; Peterson, R.M. and Wilson, K.M. (1980). Geological Ekofisk task force, Volume IIa, lithostratigraphy, sedimentology and diagenesis. Phillips Petroleum, Company Report.

Dixit, S.; Van Cappellen, P. and van Bennekom, A. Johan (2001). Processes controlling solubility of biogenic silica and pore water build-up of silicic acid in marine sediments. Marine Chemistry 73: 333–352.

Drits, V.A.; Sakharov; B.A.; Lindgreen, H. and Salyn, A. (1997). Sequential structure transformation of illite-smectite-vermiculite during diagenesis of Upper Jurassic shales from the North Sea and Denmark. Clay Minerals 32: 351–371.

Esmerode, E.V.; Lykke-Andersen, H. and Surlyk, F. (2008). Interaction between bottom currents and slope failure in the Late Cretaceous of the southern Danish Central Graben, North Sea. Journal of the Geological Society, London 165: 55–72.

Fabricius, I.L. and Borre, M.K. (2007). Stylolites, porosity, depositional texture, and silicates in chalk facies sediments. Ontong Java Plateau - Gorm and Tyra fields North Sea. Sedimentology 54: 183–205.

Fabricius, I.L., Røgen, B. and Gommesen, L. (2007). How depositional texture and diagenesis control petrophysical and elastic properties of samples from five North Sea chalk fields. Petroleum Geoscience 13: 81–95.

Farrell, H.E. (1992). XRD bulk mineral analysis: Ekofisk and West Ekofisk Fields, North Sea, Norway. Phillips Petroleum, Exploration Report no. 14612.

Fenchel, T. and Bernard, C. (1995). Mats of colourless sulphur bacteria. Major microbial processes. 128: 161–170.

Fenchel, T. and Glud, R.N. (1998). Veil architecture in a sulphide-oxidizing bacterium enhances counter current flux. Nature 394: 367–369.

Gowers, M.B. and Sæbøe, A. (1985). On the structural evolution of the Central Trough in the Norwegian and Danish sectors of the North Sea. Marine and Petroleum Geology 2: 298–318.

Hancock, J.M. (1975). The petrology of chalk. Proceedings of the Geological Association 86: 499–535.

Hancock, J.M. (1993). The formation and diagenesis of chalk, *in* Downing, R.A.; Price, M. and Jones, G.P., The hydrology of the chalk of the north-west Europe. Oxford: 14–34.

Hay, W.W. and Brock, J.C. (1992). Temporal variation in intensity of upwelling off southwest Africa, *in* Prell, C.P. and Emeis, K.C., Geological Society Special Publications. London: 463–497.

Henchiri, M. (2007). Sedimentation, depositional environment and diagenesis of Eocene biosiliceous deposits in Gafsa basin (southern Tunisia). Journal of African Earth Sciences 49: 187–200.

Hoffman, J. and Hower, J. (1979). Clay mineral assemblages as low grade metamorphic geothermometers: Application to the thrust faulted disturbed belt of Montana, U.S.A., *in* Scholle, P.A. and Schluger, P.R., Aspects of diagenesis, SEPM Special Publications. 26: 55–79.

Hower, J.; Eslinger, E.V.; Hower, M. and Perry, E.A. (1976). The mechanism of burial metamorphism of argillaceous sediments: 1. mineralogical and chemical evidence. Geological Society of America Bulletin 87: 725–737.

Iler, R.K. (1973). Effect of adsorbed alumina on the solubility of amorphous silica in water. Journal of Colloid and Interface Science 43: 399–408.

Jakobsen, F.; Lindgreen, H. and Springer, N. (2000). Precipitation and flocculation of spherical nano-silica in North Sea chalk. Clay Minerals 35: 175–184.

James, N.P. and Bone, Y. (2000). Eocene cool-water carbonate and biosiliceous sedimentation dynamics, St. Vincent Basin, South Australia. Sedimentology 47: 761–786.

Jørgensen, B.B. (1982). Mineralization of organic matter in the sea bed - the role of sulphate reduction. Nature 296: 643–645.

Jørgensen, B.B. and Revsbech, N.P. (1983). Colorless sulfur bacteria, *Beggiatoa spp*. and *Thiovulum spp*. in O_2 and H_2S microgradients. Applied and Environmental Microbiology. 45: 1261–1270.

Kastner, M. (1981). 23. Authigenic silicates in the deep-sea sediments: formation and diagenesis, *in* Emiliani, C., The Sea, New York, John Wiley & Sons. 7. The Oceanic Lithosphere: 915–980.

Kennedy, W.J. (1987). Sedimentology of Late Cretaceous-Paleocene chalk reservoirs, North Sea Central Graben, *in* Brooks, J. and Glennie, K. Petroleum Geology of the North West Europe. London, Graham and Trotman: 469–481.

Kennedy, W.J. and Garrison, R.E. (1975). Morphology and genesis of nodular chalks and hardgrounds in the Upper Cretaceous of southern England. Sedimentology 22: 311–386.

Kristensen, E. (2000). Organic matter diagenesis at the oxic/anoxic interface in coastal marine sediments, with emphasis on the role of burrowing animals. Hydrobiologia 426: 1–24.

Madsen, H.B. and Stemmerik, L. (submitted). Diagenesis of flint and porcellanite in the Maastrichtian Chalk at Stevns Klint, Denmark.

Maliva, R.G. and Dickson, J.A.D. (1992). Microfacies and diagenetic controls of porosity in Cretaceous/Tertiary chalks, Eldfisk, norwegian North Sea. The American Association of Petroleum Geologists Bulletin 76: 1825–1838.

Maliva, R.G.; Dickson, J.A.D. and Råheim, A. (1991). Modelling of chalk diagenesis (Eldfisk Field, Norwegian North Sea) using whole rock and laser ablation stable isotpoe data. Geological Magazine 128: 43–49.

Pekot, L.J. and Gregory, A.G. (1987). Ekofisk, *in* Spencer, A.M.; et al., Geology of the Norwegian oil and gas fields, London, Graham and Trotman: p. 73–87.

Sandford, F. (2003). Physical and chemical analysis of the siliceous skeletons in six sponges of two groups (demospongiae and hexactinellida). Microscopy Research and Technique 62: 336–355

Scholle, P.A. (1977). Chalk Diagenesis and Its Relation to Petroleum Exploration. The American Association of Petroleum Geologists Bulletin 61: 982–1009.

Taylor, S.R. and Lapré, J.F. (1986). North Sea chalk diagenesis: its effect on reservoir location and properties, *in* Brooks, J. and Glennie K.W. 3rd Conference on petroleum geology of North West Europe, London, England, Graham and Trotman Ltd.: p. 483-495

Ten Haven, H.L.; Little, R. and Rullkotter, J. (1990). Accumulation rates and composition of organic matter in late Cenozoic sediments underlying the active upwelling area off Peru, *in* Suess, E.; von Huene, R.; et al. Proc. ODP. 112: p. 591–605.

Vasconcelos, C. and McKenzie, J.A. (1997). Microbial mediation of modern dolomite precipitation and diagenesis under anoxic conditions (Lagoa Vermelha, Rio De Janeiro, Brazil). Journal of Sedimentary Research 67: 378–390.

Vasconcelos, C.; McKenzie, J.A.; Bernasconi, S.; Grujic, D.; Tiens, A.J. (1995). Microbial mediation as a possible mechanism for natural dolomite formation at low temperatures. Nature 377: 220–222.

von Rad, U. and Rösch, H., 1974, Petrography and diagenesis of deep-sea cherts from the central Atlantic, *in* Hsü, K.J. and Jenkyns, H.C., Pelagic sediments: on land and under the sea. Oxford, Blackwell Scientific Publications, p. 327–347.

Whitney, F.; Conway, K.W.; Thomson, R.; Barrie, J.V.; Krautter, M. and Mungov, G. (2005). Oceanographic habitat of sponge reefs on the Western Canadian Continental Shelf. Continental Shelf Research 25: 211–226.

Williams, L.A. and Crerar, D.A. (1985). Silica diagenesis, II. general mechanisms. Journal of Sedimentary Petrology 55: 312–321.

Wise, S.W. and Weaver, F.M., 1974, Chertification of oceanic sediments, *in* Hsü, K.J. and Jenkyns, H.C., Pelagic sediments: on land and under the sea: Oxford, Blackwell Scientific Publications, p. 301–326.

Wright, D.T. (2000). Benthic microbial communities and dolomite formation in marine and lacustrine environments - a new dolomite model. Marine authigenesis: from global to microbial. C. R. Glenn, L. Prévôt-Lucas and J. Lucas. Tulsa, SEPM Special Publication 66: 7–20.

Wright, D.T. and Wacey, D. (2005). Precipitation of dolomite using sulphate-reducing bacteria from the Coorong Region, South Australia: significance and implications. Sedimentology 52(5): 987–1008.

Zijlstra, H.J.P. (1987). Early diagenetic silica precipitation, in relation to redox boundaries and bacterial metabolism, in Late Cretaceous chalk of the Maastrichtian type locality." Geologie en Mijnbouw 66: 343–355.

Appendix A: XRD data of insoluble residue.

2/4-X-47		Depth				Bulk	ISR	ISR	Minerals in chalk (%)								
Plug	Core	(ft)	(inc)	Zone	Lithology	(gr.)	(gr.)	(%)	Calcite	Quartz	Kaolinite	Apatite	Dolomite	Albite	Pyrite	Crandelite	smectite-Illite
38	1	15782	3	ED	Chalk	42.81	1.88	4.4	95.6	1.7	1.0	0.3	0.2	0.6	0.6	0.1	SI
39	1	15783	3	ED	Chalk	35.37	1.32	3.7	96.3	1.5	1.2	0.2	0.3	0.3	0.3	0.0	SI
39B	1	15783	8	ED	Chalk	40.58	1.51	3.7	96.3	1.2	0.9	0.3	0.2	0.5	0.5	0.0	SI
40	1	15784	7	ED	Chalk	43.26	1.77	4.1	95.9	1.7	0.9	0.3	0.2	0.5	0.5	0.0	SI
41	1	15785	3	ED	Chalk	27.37	0.79	2.9	97.1	1.4	0.4	0.2	0.2	0.3	0.3	0.0	S
42	1	15785	7	ED	Flint												
43	1	15786	11	ED	Chalk	38.72	1.24	3.2	96.8	2.1	0.2	0.1	0.3	0.2	0.2	0.0	S
44	1	15787	1	ED	Chalk	39.2	2.15	5.5	94.5	1.7	1.5	0.4	0.2	0.8	0.8	0.0	SI
45	1	15787	6	ED	Flint												
46	1	15787	10	ED	Chalk	36.09	0.47	1.3	98.7	0.2	0.4	0.2	0.0	0.3	0.3	0.0	S
47	1	15788	6	ED	Chalk	40.83	1.27	3.1	96.9	1.3	0.4	0.1	0.7	0.2	0.2	0.0	SI
48	1	15789	3	ED	Chalk	28.03	1.03	3.7	96.3	1.0	0.9	0.2	0.4	0.6	0.6	0.0	S
49	1	15789	6	ED	Flint												
50	1	15789	11	ED	Chalk	30.94	1.07	3.5	96.5	0.8	0.9	0.3	0.2	0.6	0.6	0.0	SI
51	1	15790	4	ED	Chalk	32.34	1.12	3.5	96.5	0.8	0.0	0.3	0.7	0.8	0.8	0.0	S
52	1	15791	3	ED	Flint												
53	1	15792	7	ED	Chalk	36.86	1.22	3.3	96.7	0.8	0.0	0.3	1.0	0.6	0.6	0.0	S
54	1	15793	4	ED	Flint												
55	1	15794	5	ED	Chalk	32.45	0.92	2.8	97.2	0.5	0.0	0.2	1.4	0.3	0.3	0.0	SI
56	1	15795	2	ED	Chalk	32.83	1.51	4.6	95.4	1.3	0.0	0.5	0.7	1.0	1.0	0.0	S
56B	1	15795	4	ED	Chalk												
57	2	15796	9	ED	Chalk	36.46	1.44	3.9	96.1	1.2	0.0	0.4	0.7	0.8	0.8	0.0	S
58	2	15798	9	ED	Chalk	33.01	1.53	4.6	95.4	0.8	1.0	0.4	0.9	0.7	0.7	0.0	SI
59	2	15799	8	ED	Chalk												
60	2	15800	8	ED	Chalk	32.65	1.14	3.5	96.5	0.7	0.5	0.2	0.9	0.6	0.6	0.0	S
61	2	15801	1	ED	Flint												
62	2	15801	4	ED	Chalk	35.39	1.19	3.4	96.6	0.8	0.6	0.2	0.9	0.4	0.4	0.0	S
63	2	15802	2	ED	Flint	35.35	1.03	2.9	97.1	1.5	0.4	0.1	0.3	0.3	0.3	0.0	S
64	2	15802	3	ED	Flint												
65	2	15803	4	ED	Chalk	19.7	0.32	1.6	98.4	0.5	0.0	0.1	0.4	0.3	0.3	0.0	S
66	2	15804	5	ED	Chalk	25.33	0.82	3.2	96.8	0.8	0.7	0.2	0.6	0.5	0.5	0.0	S

Also present but not quantified ISR: insoluble residue
S:Smectite
SI: smectite-Illite

2/4-K-4		Depth				Bulk	ISR	ISR	Minerals in chalk (%)							
Plug	Core	(ft)	(inc)	Zone	Lithology	(gr.)	(gr.)	(%)	Calcite	Quartz	Kaolinite	Apatite	Dolomite	Pyrite	Crandelite	smectite-Illite
		12269	0	ED	Flint											
27		12300	0	ED	Chalk	29.73	2.3	7.7	92.3	1.0	1.1	0.3	5.2	0.0	0.0	S
3		12304	6	ED	Chalk	20.42	1.63	8.0	92.0	2.1	0.8	0.3	4.7	0.0	0.0	S
2		12305	1	ED	Chalk	30.45	1.78	5.8	94.2	2.4	0.7	0.2	2.6	0.0	0.0	S
1		12305	3	ED	Chalk	27.96	0.37	1.3	98.7	0.6	0.3	0.1	0.4	0.0	0.0	S
6		12307	9	EE	Chalk	35.99	8.04	22.3	77.7	7.8	13.3	0.7	0.4	0.1	0.0	SI
5		12307	11	EE	Chalk	36.79	6.53	17.7	82.3	6.9	9.5	0.7	0.5	0.1	0.0	SI
4		12308	9	EE	Chalk	23.16	1.88	8.1	91.9	2.5	1.0	0.4	4.2	0.0	0.0	S
24		12309	6	EE	Marl	50.7	28.46	56.1	43.9	6.6	46.9	2.0	0.0	0.7	0.0	SI
12		12351	1	EE	Marly chalk	34.65	17.57	50.7	49.3	30.3	15.5	1.8	2.8	0.4	0.0	S
8		12351	9	EE	Chalk	24.74	12.88	52.1	47.9	16.7	21.8	0.0	12.8	0.7	0.0	S
9		12355	2	EE	Chalk	33.17	22.07	66.5	33.5	33.2	25.9	0.0	6.7	0.7	0.0	S
15		12357	0	EE	Chalk	27.35	19.71	72.1	27.9	37.3	23.5	2.6	8.1	0.5	0.0	S
10		12357	3	EE	Marl	24.99	18.08	72.3	27.7	31.3	35.9	2.6	0.0	2.6	0.0	S
13		12357	6	EE	Marl	31.37	21.61	68.9	31.1	33.7	28.5	0.0	6.0	0.6	0.0	S
7		12357	10	EE	Chalk	36.91	23.46	63.6	36.4	21.4	31.1	0.0	11.0	0.0	0.0	SI
		12358	0	EE	Flint											
11		12359	7	EE	Chalk	29.9	5.54	18.5	81.5	13.0	4.2	0.6	0.5	0.1	0.0	S
		12359	11	EE	Flint											
16		12360	0	EE	Chalk	34.37	1.67	4.9	95.1	2.3	1.6	0.4	0.5	0.2	0.0	S
26		12361	6	EE	Chalk	44.07	5.9	13.4	86.6	7.1	4.6	0.6	0.9	0.1	0.0	S
		12362	1	EE	Flint											
14		12367	0	EE	Chalk	23.35	5.21	22.3	77.7	10.3	9.9	1.1	0.8	0.3	0.0	S
21		12367	8	EE	Chalk	28.75	7.77	27.0	73.0	12.4	14.1	0.0	0.0	0.6	0.0	SI
17		12369	3	EE	Chalk	19.34	5.31	27.5	72.5	10.3	16.9	0.0	0.0	0.3	0.0	SI
19		12369	7	EE	Chalk	63.63	21.5	33.8	66.2	11.9	21.5	0.0	0.0	0.3	0.0	S
22		12370	3	EE	Chalk	59.22	6.61	11.2	88.8	4.8	5.1	0.0	0.0	0.2	1.1	SI
20		12370	7	EE	Chalk/Marl	34.09	16.98	49.8	50.2	21.6	27.4	0.0	0.0	0.8	0.0	SI
18		12373	6	EE	Chalk	58.21	7.26	12.5	87.5	6.2	5.8	0.4	0.0	0.1	0.0	S
25		12374	10	EE	Chalk	31.63	2.79	8.8	91.2	2.2	5.7	0.5	0.3	0.2	0.0	S
		12375	11	EE	Flint											
23		12378	11	EE	Chalk	35.84	4.8	13.4	86.6	7.4	5.9	0.0	0.0	0.1	0.0	S

Also present but not quantified ISR: insoluble residue
S:Smectite
SI: smectite-Illite

2/4-X-32 Plug	Core	Depth (ft)	(inc)	Zone	Lithology	Bulk (gr.)	ISR (gr.)	ISR (%)	Minerals in chalk (%) Calcite	Quartz	Kaolinite	Apatite	Dolomite	Pyrite	smectite-Illite
1	1	10640	3	EE	Chalk	35.18	17.48	56.3	50.3	25.1	20.6	0.0	3.5	0.6	
2	1	10640	11	EE	Chalk	27.51	4.87	17.7	82.3	4.9	9.7	1.1	1.7	0.3	
3	1	10641	10	EE	Chalk	27.5	19.73	71.7	28.3	42.8	21.5	0.0	6.9	0.6	S
4	1	10643	5	EE	Chalk	28.48	11.53	40.5	59.5	25.6	12.3	0.0	2.3	0.3	S
5	1	10644	4	EE	Chalk	26.76	9.18	34.3	65.7	22.2	11.6	0.0	0.0	0.5	S
6	1	10645	3	EE	Chalk	25.86	17.11	66.2	33.8	40.7	24.6	0.0	0.0	0.8	
7	1	10645	5	EE	Marl	30.76	13.82	44.9	55.1	6.9	30.2	2.6	3.8	1.4	SI
8	1	10645	8	EE	Flint										
9	1	10646	3	EE	Flint										
10	1	10646	8	EE	Chalk	33.05	2.9	8.8	91.2	6.1	0.0	1.3	1.2	0.3	
11	1	10646	11	EE	Flint										
12	1	10647	3	EE	Chalk	30.22	2.86	9.5	90.5	5.6	2.7	0.5	0.5	0.1	SI
13	1	10647	8	EE	Chalk	27.36	4.71	17.2	82.8	12.1	3.8	0.7	0.6	0.1	SI
14	1	10648	9	EE	Chalk	37.29	6.09	16.3	83.7	7.6	4.3	0.1	4.2	0.2	
15	1	10649	3	EE	Chalk	25.43	19.81	77.9	22.1	45.4	31.4	0.0	0.0	1.1	SI
15B	1	10649	6	EE	Marl	26.63	23.03	86.5	13.5	31.1	48.9	4.4	0.0	2.1	SI
16	1	10649	10	EE	Chalk	31.03	8.58	27.7	72.3	21.9	0.0	0.0	5.3	0.4	S
17	1	10650	10	EE	Chalk	27.22	18.78	69.0	31.0	31.5	36.3	0.0	0.0	1.3	SI
18	1	10651	10	EE	Chalk	30.89	18.27	59.1	40.9	39.1	17.6	1.9	0.0	0.6	S
19	1	10652	2	EE	Marl	32.84	24.35	74.1	25.9	33.5	35.8	3.6	0.0	1.2	SI
20	1	10652	5	EE	Chalk	12.63	3.14	24.9	75.1	19.0	0.0	0.0	0.0	5.8	
21	1	10652	9	EE	Chalk	28.19	4.02	14.3	85.7	12.7	0.0	0.7	0.8	0.1	S
22	1	10652	11	EE	Flint										
23	1	10653	4	EE	Chalk	37.86	10.24	27.0	73.0	10.5	12.9	1.4	1.9	0.4	SI
24	1	10653	7	EE	Chalk	35.85	3.84	10.7	89.3	5.8	3.8	0.0	1.0	0.1	S
25	1	10653	9	EE	Chalk	33.11	2.9	8.8	91.2	5.5	0.0	1.1	2.0	0.2	S
26	1	10654	0	EE	Flint	27.05	2.15	7.9	92.1	6.9	0.0	1.0	0.0	0.1	S
26B	1	10654	2	EE	Flint										
27	1	10655	2	EE	Flaser chalk	39.27	2.71	6.9	93.1	4.0	0.0	0.6	2.2	0.1	SI
28	1	10655	10	EE	Flaser chalk	34.12	6.62	19.4	80.6	10.6	7.3	1.0	0.0	0.5	S
29	1	10656	8	EE	Flaser chalk	37.58	19.14	50.9	49.1	21.8	24.3	2.2	1.9	0.8	SI
30	1	10657	5	EE	Chalk	36.1	1.03	2.9	97.1	1.2	1.2	0.2	0.2	0.0	SI
31	1	10658	4	EE	Chalk	33.13	1.52	4.6	95.4	2.0	2.1	0.2	0.3	0.0	SI
32	1	10659	4	EE	Flaser chalk	30.86	5.68	18.4	81.6	9.9	7.2	0.6	0.5	0.2	SI
33	1	10659	11	EE	Chalk/Flint	37.76	0.69	1.8	98.2	0.9	0.8	0.1	0.0	0.0	SI
34	1	10660	0	EE	Flint										
35	1	10660	4	EE	Chalk	32.06	0.77	2.4	97.6	1.3	0.8	0.2	0.1	0.0	SI
36	2	10662	7	EE	Chalk	39.15	7.16	18.3	81.7	9.5	7.8	0.8	0.0	0.2	SI
37	2	10665	4	TA	Chalk	30.55	3.09	10.1	89.9	7.6	2.1	0.3	0.0	0.1	S

Also present but not quantified ISR: insoluble residue
S:Smectite
SI: smectite-Illite

2/4-A-6		Depth				Bulk	ISR	ISR	Minerals in chalk (%)								
Plug	Core	(ft)	(inc)	Zone	Lithology	(gr.)	(gr.)	(%)	Calcite	Quartz	Kaolinite	Apatite	Dolomite	Pyrite	Crandelite	Barite	smectite-Illite
1		11465	4	ED	Chalk	40.51	1.99	4.9	95.1	1.3	1.2	0.2	2.1	0.0	0.0	0.1	S
2		11464	10	ED	Chalk	41.96	1.99	4.7	95.3	1.3	1.7	0.3	1.4	0.1	0.0	0.0	SI
3		11465	6	ED	Flint												
4		11478	0	EE	Chalk	35.58	1.92	5.4	94.6	2.1	1.7	0.3	1.1	0.1	0.0	0.0	S
5		11478	6	EE	Chalk	28.29	1.85	6.5	93.5	2.4	1.9	0.4	1.8	0.1	0.0	0.0	S
6		11479	2	EE	Chalk	35.93	3.38	9.4	90.6	4.2	2.7	0.4	1.8	0.1	0.0	0.1	S
7		11480	0	EE	Chalk	40.09	0.46	1.1	98.9	0.3	0.5	0.1	0.3	0.0	0.0	0.0	SI
8		11480	4	EE	Flint												
9		11480	7	EE	Chalk	64.77	11.9	18.3	81.7	9.0	6.8	1.2	1.4	0.0	0.0	0.0	SI
10		11480	10	EE	Flint												
11		11481	2	EE	Chalk	46.44	17.5	37.7	62.3	4.8	28.9	0.0	0.0	0.5	3.5	0.0	SI
12		11482	1	EE	Chalk	29.94	4.26	14.2	85.8	7.2	5.3	0.7	0.6	0.4	0.0	0.0	S
13		11482	11	EE	Chalk	34.57	7.9	22.9	77.1	7.3	14.6	0.7	0.0	0.2	0.0	0.0	SI
14		11529	0	EE	Chalk	41.42	4.82	11.6	88.4	5.9	4.1	0.5	1.0	0.1	0.0	0.0	
15		11529	11	EE	Chalk	30.34	21.1	69.4	30.6	26.5	40.8	0.0	0.0	2.0	0.0	0.0	
16		11530	8	EE	Chalk	37.42	4.12	11.0	89.0	3.8	5.0	0.0	2.0	0.2	0.0	0.0	S
17		11532	4	EE	Chalk	17.99	7.06	39.2	60.8	16.4	17.3	1.8	3.2	0.5	0.0	0.0	SI
18		11532	11	EE	Chalk	49.31	20.5	41.6	58.4	14.3	15.3	0.0	11.0	0.9	0.0	0.0	S
19		11533	2	EE	Marl	38.71	25.9	66.9	33.1	22.7	27.6	3.1	12.6	0.9	0.0	0.0	SI
20		11534	2	EE	Chalk	33.46	1.76	5.3	94.7	1.9	2.8	0.2	0.3	0.0	0.0	0.0	
21		11534	9	EE	Chalk	31.41	1.52	4.8	95.2	2.3	2.0	0.2	0.4	0.0	0.0	0.0	S
22		11534	11	EE	Chalk	28.53	1.51	5.3	94.7	2.3	2.5	0.2	0.3	0.0	0.0	0.0	S
23		11536	0	TA	Chalk	32.2	0.78	2.4	97.6	0.9	1.0	0.3	0.1	0.0	0.0	0.0	S
24		11537	3	TA	Chalk	37.37	1.99	5.3	94.7	2.6	1.7	0.3	0.6	0.1	0.0	0.0	S
25		11538	3	TA	Chalk	28.42	1.06	3.7	96.3	1.5	1.5	0.3	0.4	0.0	0.0	0.0	S
26		11538	10	TA	Chalk	32.07	1.34	4.2	95.8	1.6	1.7	0.3	0.4	0.0	0.0	0.0	S
27		11539	0	TA	Chalk	18.87	0.75	4.0	96.0	2.0	1.4	0.2	0.3	0.0	0.0	0.0	S
28		11540	0	TA	Chalk	32.16	1	3.1	96.9	1.1	1.4	0.3	0.3	0.0	0.0	0.0	
29		11540	10	TA	Chalk	32.09	0.99	3.1	96.9	1.1	1.6	0.2	0.2	0.0	0.0	0.0	S
30		11541	3	TA	Chalk	32.38	1.12	3.5	96.5	1.4	1.3	0.2	0.4	0.0	0.0	0.1	S
31		11542	3	TA	Chalk	23.62	1.01	4.3	95.7	1.7	1.7	0.3	0.5	0.0	0.0	0.1	S
32		11543	1	TA	Chalk	43.58	1.58	3.6	96.4	1.7	1.4	0.2	0.3	0.0	0.0	0.0	S
33		11544	10	TA	Chalk	49.92	2.18	4.4	95.6	0.8	2.7	0.3	0.3	0.1	0.0	0.2	S
34		11546	8	TA	Chalk	39.64	1.38	3.5	96.5	1.4	1.5	0.2	0.3	0.0	0.0	0.0	
35		11559	0	TA	Chalk	56.46	2.03	3.6	96.4	1.0	1.1	0.3	1.1	0.0	0.0	0.1	S
36		11559	6	TA	Chalk	15.5	0.46	3.0	97.0	1.1	1.3	0.2	0.3	0.0	0.0	0.0	S
37		11560	6	TA	Chalk	28.92	1.14	3.9	96.1	1.1	0.9	0.2	1.7	0.0	0.0	0.0	S

Also present but not quantified ISR: insoluble residue
S:Smectite
SI: smectite-Illite

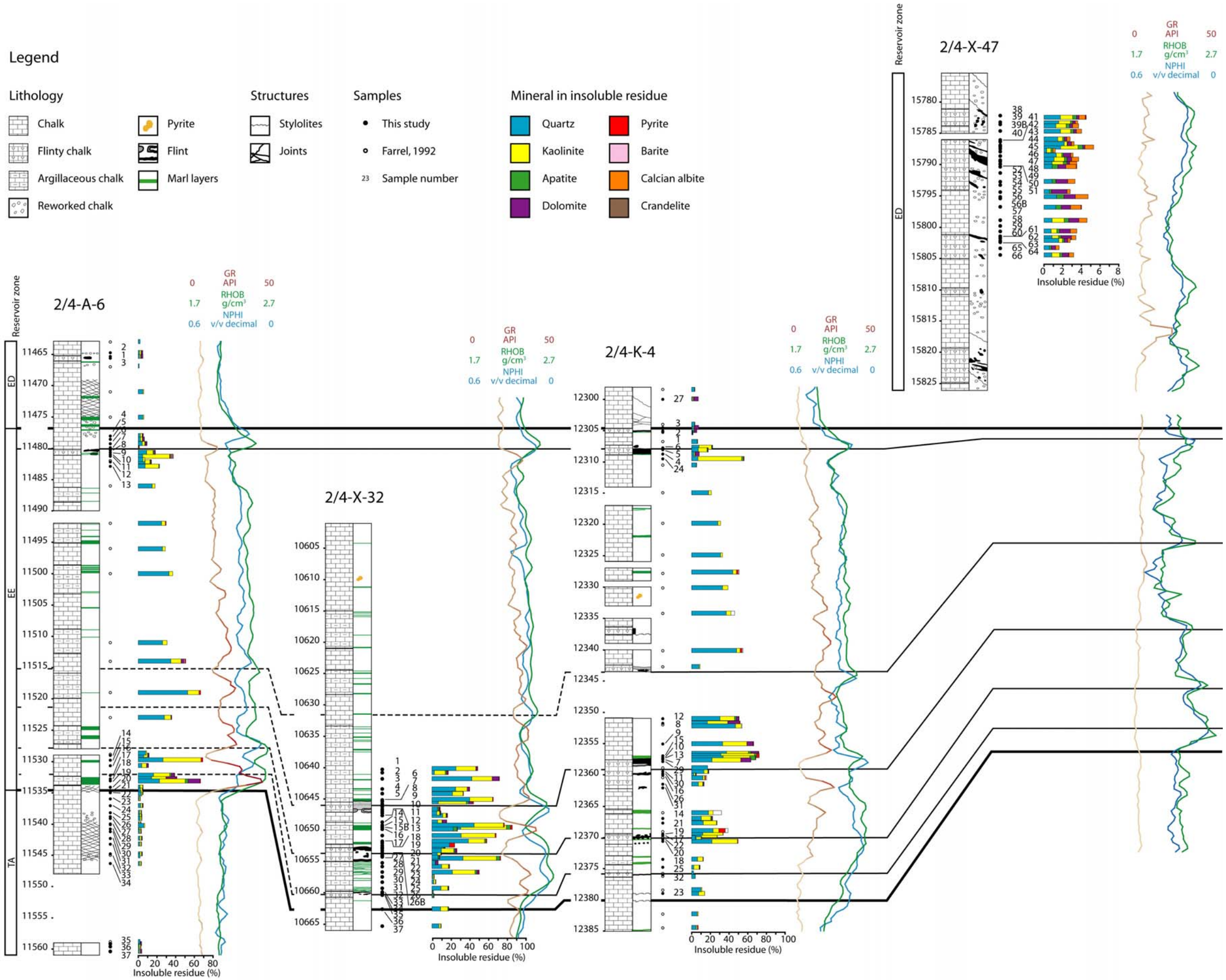

Figur 3 Petrophysical logs, lithology and mineralogy of the chalk in the 2/4-X-47, 2/4-K-4, 2/4-X-32 and 2/4-A-6 cores. Correlations between zone boundaries are marked with thick lines, flint layers are marked with thin lines. Silicified horizons are correlated with flint layers and are marked with broken lines. Length of bars illustrates the amount of insoluble residue and the colours represent the content of different minerals according to the legend.

Appendix B: Log correlation of wells 2/4-X-47, 2/4-K-4, 2/4-X-32, 2/4-A-6, 2/4-4 and 2/7-B-12 A.